Evaluation of Operational Reliability of a Microgrid Using a Short-Term Outage Model

Xufeng Xu, Joydeep Mitra, *Senior Member, IEEE*, Tingting Wang, *Student Member, IEEE*, and Longhua Mu

***Abstract*—Island-capable microgrids can potentially improve customer reliability, but protection-related issues can adversely affect this reliability benefit. At the same time, average annualized indices often do not effectively convey a complete picture of load-point reliabilities in microgrids integrated with multiple weather-dependent microsources. The primary goal of this work is to investigate the impacts of protection system and operating conditions on the reliability indices of a microgrid. The proposed method utilizes a short-term outage model that quantifies the relationship between state variables and the outage rate of component. A hybrid approach is proposed, which combines scenario selection and enumerative analysis. Simulations on a test system illustrate the dependence of operational reliability on factors such as local meteorological conditions, correlation between variable generation and loads, as well as the effects of protection system operations. Finally, some recommendations on the parameter settings of protection system are provided to enhance the system reliability.**

***Index Terms*—Microgrid, microsource, operating condition, protection system, reliability, short-term outage model.**

I. Introduction

THE penetration of microgrids has been on the rise in recent years. While this phenomenon has been driven by many factors, such as deployment of small-scale energy sources including renewables, and avoidance of transmission and distribution expansion, perhaps the most compelling consideration has been that of reliability. The availability of microsources (μS) at or near load points not only provide the obvious benefits of both interruption rate and its duration [1], but also open up the possibility of offering reliability- differentiated services.

Some researchers regard microgrid as a distribution system with embedded μSs, which may operate in grid-connected or islanded mode. Therefore, indices defined for distribution system are still employed to assess microgrid reliability [2]–[4]. However, microgrid has unique characteristics in structure compared with distribution system [5]. Thus, a series of new metrics specially designed for microgrid reliability is necessary and [6] is such an example.

On the other hand, many μSs in microgrid are intermittent and their outputs are closely related to weather conditions, such as wind speed and solar radiation intensity. Therefore, the available power of μSs for load recovery remains uncertain after failure events. In [7], the contribution of wind energy to the reliability improvement is quantified based on the site conditions. Similarly, in [8], the hourly mean solar radiation is used to analyze the reliability of a single generation system. In addition, storage is a vital part of microgrid, and the integration energy storage system could significantly mitigate the negative influence of interruption [2], [9].

The existing literature related to microgrid reliability has mainly focused on two aspects:

1) *Reliability Evaluation of Distribution System with Microgrids* [1], [10]. Microgrid point is distinct from load point or traditional generation point. Therefore, the reliability assessment of a distribution system with embedded μSs necessitates development of a suitable modeling and analysis method for the microgrid. For example, a new concept, namely, virtual power plant, is introduced to model microgrids in [10].
2) *Reliability Assessment of Microgrid System* [2]–[4], [6], [11]. Compared with distribution systems, the restoration process of microgrids after outage possesses its own characteristics and the diversified ownerships of μSs should be given due consideration. Microgrid operator is not responsible for the customer who has no contract with the microgrid. In other words, customers may be treated unfairly in the restoration process.

However, previous studies have failed to consider the effects of microgrid protection on reliability evaluation process. Protection problem is still an important issue which should be properly resolved in a microgrid. Incorrect actions of protective devices will reduce reliability of service. Moreover, the increase in transfer capacity of a feeder will amplify its failure probability [12]. We propose an efficacious approach to achieve accurate reliability indices while considering the state-of-the-art technical level of microgrid protection.

The remainder of this paper is organized as follows: in Section II, the grid mesh method is proposed to deal with the scenario selection problem. Section III establishes the short-term outage model for main feeder and lateral distributor.

Manuscript received June 27, 2013; revised September 24, 2013 and December 20, 2013; accepted January 28, 2014. This work was supported in part by the Shanghai Natural Science Fund for Youth Scholars (12ZR1451300), in part by the Specialized Research Fund for the Doctoral Program of Higher Education (20120072120045), and in part by the Fundamental Research Funds for the Central Universities (2012KJ003). Paper no. TPWRS-00834-2013.

X. Xu is with the Department of Electrical Engineering, Tongji University, Shanghai 201804, China (e-mail: xfxu@tongji.edu.cn)

J. Mitra is with Michigan State University, East Lansing, MI 48824 USA (e-mail: mitraj@msu.edu).

T. Wang is with Clemson University, Clemson, SC 29631 USA (e-mail: twang@clemson.edu).

L. Mu is with Tongji University, Shanghai 201804, China (e-mail: lhmu@tongji.edu.cn).

Color versions of one or more of the figures in this paper are available online at http://ieeexplore.ieee.org.

Digital Object Identifier 10.1109/TPWRS.2014.2303792

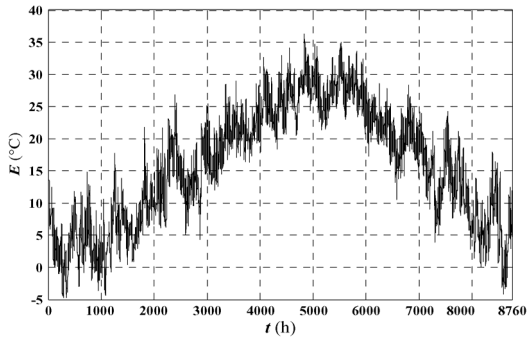

Fig. 1. Hourly environmental temperature of a district located in Eastern China in a specified year.

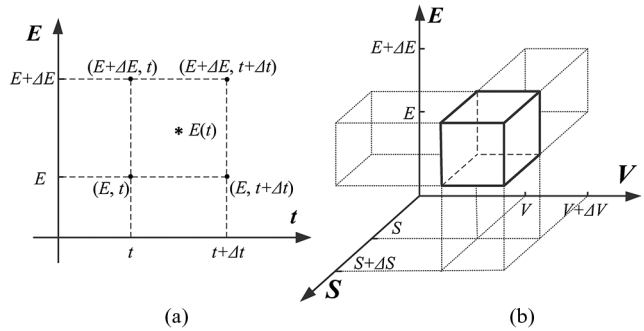

Fig. 2. Partitioning of the state space. (a) Two-dimensional space. (b) Three-dimensional space.

An enumerative analysis based hybrid approach is developed in Section IV for the calculation of short-term reliability indices. A case study is employed in Section V to illustrate the performance of the proposed model and assessment approach. Section VI provides some concluding remarks.

II. Modeling of Microsources

μSs are usually viewed as alternative power sources after failure events. Therefore, their available capacities will significantly influence customer reliability. However, many μSs in microgrid are weather-dependent and their power outputs are characterized as intermittent and even unpredictable. Here, two widely installed μSs, namely photovoltaic (PV) arrays and wind turbine generator (WTG) respectively, are considered as two examples to address this problem.

The output of a photovoltaic array relies on its rated power G_{rate}, illumination S and environmental temperature E [13]

$$G_S = \frac{S}{S_{rate}} \cdot \eta(E) \cdot G_{rate} \tag{1}$$

$$\eta(E) = 1 - 0.0045 \cdot (E - E_{rate}) \tag{2}$$

where S_{rate} is the rated value of solar radiation, efficiency factor $\eta(E)$ is defined to quantify the impacts of E, and reference temperature E_{rate} is commonly set to 25°C.

Similarly, wind turbine generator delivers rated power G_{rate} only when the wind speed is within a special interval. Its operation modes can generally be divided into three stages according to the wind speed V [14]

$$G_W = \begin{cases} G_{rate}, & V_{rate} \le V < V_{co} \\ \frac{G_{rate}(V - V_{ci})}{V_{rate} - V_{ci}}, & V_{ci} \le V < V_{rate} \\ 0, & \text{otherwise} \end{cases} \tag{3}$$

where V_{ci}, V_{co} and V_{rate} are the cut-in wind speed, the cut-out wind speed and the rated wind speed, respectively.

Due to the unprecise weather forecasting technology, the available power of μSs remains uncertain during the planning horizon. However, annual meteorological data follow a statistical regularity. Fig. 1 shows the hourly environmental temperature $E(t)$ of H town located in Eastern China in a specified year based on historical data.

All historical data including E, S and V can be obtained from local meteorological department. Their combination is defined as a scenario which is represented by σ:

$$\sigma = \{E(t), S(t), V(t)\}\,. \tag{4}$$

They are usually recorded per minute or several minutes in the meteorological database. Therefore, the number of scenarios N_σ is an extremely large value. To relieve the computational load of the proposed model, a grid mesh method is employed in each hour-period to implement scenario reduction.

First, the two-dimensional space in Fig. 1 is divided in the following way:

- The horizontal axis is divided into short periods (Δt) which should not be less than the sampling time interval.
- The partition of the vertical axis is implemented by individual step lengths represented by ΔE.

Second, a value $E(t)$ is deployed for the rectangular space shown in Fig. 2(a). All sampling values of temperature within this space are set to $E(t)$. Similarly, illumination $S(t)$ and wind speed $V(t)$ are handled in the same way.

Subsequently, the three-dimensional space in Fig. 2(b) is divided into several cuboids. Each cuboid corresponds to a scenario σ and only those cuboids with sampling values are included in an hourly scenario set Ω_t. If scenario σ_k has sampling values of $n(\sigma_k)$, then

$$\sum_{\sigma_k \in \Omega_t} n(\sigma_k) = \frac{1}{\Delta t}, \quad (k = 1, 2, \ldots, n_t) \tag{5}$$

where n_t is the kinds of scenario in Ω_t.

Assuming Ω is annual scenario set, and N_σ is the total number of scenarios, they are calculated as

$$\Omega = \Omega_1 \cup \Omega_2 \cup \cdots \Omega_{8760} \tag{6}$$

$$N_\sigma = \sum_{t=1}^{8760} n_t. \tag{7}$$

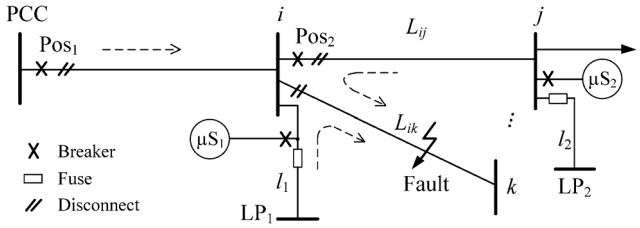

Fig. 3. Part of microgrid system.

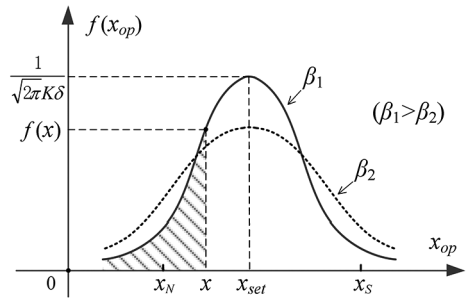

Fig. 4. Probability density function of the trigger value.

III. Short-Term Outage Model

A. Characteristics of Microgrid Protection

In microgrid, circuit breaker is commonly installed at point of common coupling (PCC) and the interface points of μSs, as shown in Fig. 3. Compared with breaker, fuse is used much more often as an additional protection and it is usually deployed at the tie point in each lateral distributor.

The protection system isolates failure component so as to limit failure impacts. However, μSs in microgrid have negative influences on the operations of protective devices including rejection and malfunction. When a short circuit fault occurs on the feeder L_{ik}:

- The short circuit current through the main protective relay at Pos_1 may be smaller than its setting value. Consequently, the relay refuses to operate.
- Protection device at Pos_2 may respond to the fault, resulting in maloperation.

The problem of effective protective strategies continues to be a topic of active research. This section will analyze the effects of microgrid protection on customer reliability.

B. Failures on Main Feeder

Remark 1: A virtual setting value x_{set} is introduced for each main feeder. It is different from the trigger value x_{op}. The protection system operates only when state variable x is larger than x_{op}.

It is assume that x_{op} follows a truncated normal distribution and its mean value is set to x_{set}. The probability density function of x_{op} is

$$f(x_{op}) = \frac{1}{\sqrt{2\pi}\delta K} \cdot \exp\left[-\frac{(x_{op}-x_{set})^2}{2\delta^2}\right], \quad x_{op} \in [0,+\infty). \tag{8}$$

Since $\int_0^{+\infty} f(x_{op})\mathrm{d}x_{op} = 1$, $K = \Phi(x_{set}/\delta)$, where $\Phi(\cdot)$ is the cumulative distribution function of standard normal distribution.

Furthermore, three parameters are introduced to describe characteristics of microgrid protection.

Definition 1: Sensitivity factor α is defined to characterize the ratio relationship between virtual setting value x_{set} and normal rating value x_N.

The ratio α, defined as "x_{set}/x_N", is used to measure the dependence of the protection system on state variables, such as voltage and current. Since x_{set} is a virtual value, another variable x_S is introduced to limit its range. In this paper, the short term rating value, which indicates the feeder's capability to handle a short term operation following contingencies, is chosen as x_S. For instance, x_N and x_S are the rated current and maximum allowable current, respectively, when referring to current protection. Thus, α lies within the interval $(1, x_S/x_N)$.

Definition 2: Accuracy factor β is defined to measure the action zone of the protective device

$$\beta = \frac{x_S - x_N}{\delta}. \tag{9}$$

Since variance δ determines the amount of dispersion, the curve shape of $f(x_{op})$ is dependent on β, as shown in Fig. 4.

If x_{set}/δ is larger than 3, then

$$\int_0^{2x_{set}} f(x_{op})\mathrm{d}x_{op} > 0.997. \tag{10}$$

Thus, K can be regarded as 1 when $\alpha\beta \cdot x_N/(x_S - x_N)$ is greater than 3.

Definition 3: Reliability factor γ is defined as the annual probability of incorrect actions of microgrid protection, which includes both malfunction and rejection $(0 < \gamma < 1)$.

Consider the following three events related to the protective device:

A	$x \geq x_{op}$ (protection operates), shown as the shaded area in Fig. 4;
$\overline{\mathrm{A}}$	$x < x_{op}$ (no action);
B	incorrect operation of protective device.

Assuming $P_{rej}(x)$ is the conditional probability of rejection and $P_{mal}(x)$ is the conditional probability of malfunction

$$\begin{aligned} P_{inc}(x) &= \Pr\{\mathrm{A}\} \cdot \Pr\{\mathrm{B}|\mathrm{A}\} + \Pr\{\overline{\mathrm{A}}\} \cdot \Pr\{\mathrm{B}|\overline{\mathrm{A}}\} \\ &= \Pr(x \geq x_{op}) \cdot P_{rej}(x) + \Pr(x < x_{op}) \cdot P_{mal}(x) \\ &= \int_0^x f(x_{op})\mathrm{d}x_{op} \cdot P_{rej}(x) + \int_x^{+\infty} f(x_{op})\mathrm{d}x_{op} \cdot P_{mal}(x) \end{aligned} \tag{11}$$

where $P_{inc}(x)$ is approximately equal to "$\gamma\Delta t/8760$", which represents the average probability of incorrect operations in a short-term Δt.

When $x \in [0, x_N]$, $\int_0^x f(x_{op})\mathrm{d}x_{op}$ is much less than $\int_x^{+\infty} f(x_{op})\mathrm{d}x_{op}$. Furthermore, $P_{rej}(x)$ is negligible if the backup protection is considered. Equation (12) is derived:

$$P_{inc}(x) \approx \int_x^{+\infty} f(x_{op})\mathrm{d}x_{op} \cdot P_{mal}(x). \tag{12}$$

Thus, the operation probability of protective device $P(x)$ in Δt is calculated as

$$\begin{aligned} P(x) &= \int_0^x f(x_{op})\mathrm{d}x_{op} \cdot [1 - P_{rej}(x)] + \int_x^{+\infty} f(x_{op})\mathrm{d}x_{op} \cdot P_{mal}(x) \\ &\approx \int_0^x f(x_{op})\mathrm{d}x_{op} + \frac{\gamma \cdot \Delta t}{8760}. \end{aligned} \tag{13}$$

$P(x)$ contains two items: one is related to the correct action when state variable exceeds the trigger value; the other is caused by the malfunction of protection.

For a feeder that has been in operation until time T, its outage probability in the next incremental Δt is given

$$\begin{aligned} \Pr(T \le t \le T + \Delta t | t > T) &= \frac{\Pr\left[(T \le t \le T + \Delta t) \cap (t > T)\right]}{\Pr(t > T)} \\ &= \frac{\Pr(T \le t \le T + \Delta t)}{\Pr(t > T)} \\ &= \lambda \cdot \Delta t + o(\Delta t). \end{aligned} \tag{14}$$

In (14), λ is the short-term outage rate of the feeder and it determines the probability of a failure transition in Δt. Assume that Δt is of the same order of magnitude as the repair time of the feeder, the probability of multiple failure events occurring on the same feeder during Δt is negligible, i.e., the infinitesimal quantity of higher order $o(\Delta t)$ is negligible.

On the other hand, the outage probability in Δt is the sum of $P(x)$ and random failure probability. Let λ_0 be annual outage rate of component, $\lambda(x)$ may be approximated as follows:

$$\lambda(x) \approx \frac{P(x) + \left(\lambda_0 \cdot \frac{\Delta t}{8760}\right) \cdot \Delta t}{\Delta t} = \frac{P(x)}{\Delta t} + \lambda_0 \cdot \frac{\Delta t}{8760}. \tag{15}$$

It should be noted that the second term in (15) corresponding to random failure is not negligible.

In this study, voltage deviation ΔU and current amplitude I are chosen as the state variable x. Thus, λ is evaluated in line with (17):

$$\Delta U = \frac{|U - U_N|}{U_N} \times 100\% \tag{16}$$

$$\lambda = \max\left\{\lambda(\Delta U), \lambda(I)\right\}. \tag{17}$$

C. Failures on Lateral Distributor

According to the mean time to failure, outages that occur on lateral distributor are divided into three categories: random failure (I), outages caused by fuse operation (II) and instantaneous aging (III), as shown in Fig. 5.

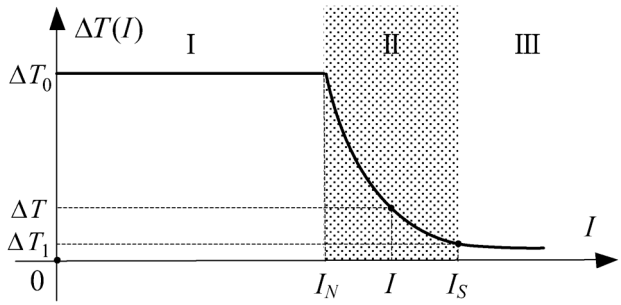

Fig. 5. Time to failure of a lateral distributor.

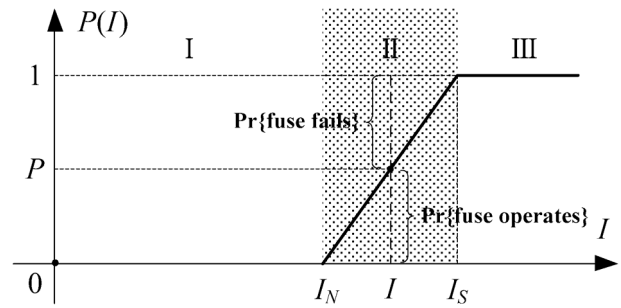

Fig. 6. Operation probability of fuse protection.

Fuse operation is caused by abnormal temperature increase which is fundamentally due to over-current through the lateral distributor. Therefore, the action time ΔT is proportional to heat or $\Delta T \propto I^2$. We assume that ΔT is expressed by a generalized formula

$$\Delta T(I) = \kappa(I - I')^{-2} + \Delta T', \quad I_N \le I \le I_S. \tag{18}$$

Since $\Delta T \to 0$ if $I \to \infty$, $\Delta T' = 0$. Furthermore, the curve of function $\Delta T(I)$ in Fig. 5 travels through points $(I_N, \Delta T_0)$ and $(I_S, \Delta T_1)$. Parameters κ and I' can be calculated as follows:

$$\kappa = \Delta T_0 \Delta T_1 \left(\frac{I_S - I_N}{\sqrt{\Delta T_0} - \sqrt{\Delta T_1}}\right)^2 \tag{19}$$

$$I' = \frac{\sqrt{\Delta T_0} \cdot I_N - \sqrt{\Delta T_1} \cdot I_S}{\sqrt{\Delta T_0} - \sqrt{\Delta T_1}} \tag{20}$$

where ΔT_0 represents the mean time to failure in normal condition (MTTF) and ΔT_1 is the melting time when $I = I_S$.

On the other hand, the probability of fuse operation in the short period Δt is mathematically described in (21) and graphically illustrated in Fig. 6:

$$P(I) = \begin{cases} 0, & I < I_N \\ \frac{I - I_N}{I_S - I_N}, & I_N \le I \le I_S \\ 1, & I > I_S. \end{cases} \tag{21}$$

Similar to the analysis on the feeder, the short-term outage rate of the lateral distributor also contains two parts: fuse operation and random failure

$$\lambda(I) = \frac{P(I)}{\Delta T(I)} + \lambda_0 \cdot \frac{\Delta t}{8760}. \tag{22}$$

Given the repair process of the lateral distributor, only one failure event is considered during Δt even if $\Delta T < \Delta t$; hence, (22) is modified as follows:

$$\lambda(I) = \frac{P(I)}{\max\{\Delta T(I), \Delta t\}} + \lambda_0 \cdot \frac{\Delta t}{8760}. \tag{23}$$

The failure on the lateral distributor will contribute to the reliability indices of load points: 1) For the load point supplied by this distributor, its average outage rate is summarized by $\lambda(I)$ in (23). 2) Occasionally, the fuse fails to operate with a probability "$1 - P(I)$" when it is supposed to protect the distributor, as shown in Fig. 6. In this case, the backup protection functions and eventually causes the outages of some load points in other lateral distributors, as measured by (24):

$$\begin{aligned}\lambda'(I) &= (\text{failure rate} \mid \text{fuse operates}) \times \Pr\{\text{fuse operates}\} \\ &\quad + (\text{failure rate} \mid \text{fuse fails}) \times \Pr\{\text{fuse fails}\} \\ &= 0 \times P(I) + \lambda(I) \times [1 - P(I)] \\ &= \lambda(I) \times [1 - P(I)]. \end{aligned} \tag{24}$$

IV. Enumerative Analysis

In addition to the outage rate of customer, μSs can shorten the average outage times at some load points.

A. Classification of Load Points

All failures types which have a contribution to the failure of any load point are enumerated. Load point LP_i is classified into three categories according to its outage time r_{ie} in a failure event τ_e ($i = 1, 2, \ldots, N$, $e = 1, 2, \ldots, M$, N and M are the number of load points and the number of failure events, respectively):

1) $r_{ie} = 0$: LP_i has no load lost.
2) $r_{ie} = t_d$ (t_d is the isolation time): LP_i can be transferred through μS or the normally open transfer point.
3) $r_{ie} = t_r$ (t_r is the repair time): LP_i will lose power until fault recovery.

If it is impossible to transfer all demands at a load point, the outage time of this load point is approximated by

$$r_{ie} = (1 - x_i\%) \cdot t_r + x_i\% \cdot t_d \tag{25}$$

where $x_i\%$ is the percentage of recovered load.

B. Heuristic Sequence Approach for Load Recovery

There is a restriction on the load amount that can be transferred through μSs or the normally open transfer point. Two priority rules are used in determining the load recovery sequence: electrical distance and load importance. It is attempted to first restore an important load point that is within a short electrical distance of an alternative power source. The electrical distance Z_{ij} is defined as the accumulated value of series impedances of the feeders between LP_i and alternative power source G_j:

$$Z_{ij} = \sum_{l \in \Lambda} (R_l + jX_l) \tag{26}$$

where R_l and X_l are the resistance and reactance of feeder l; Λ is the set of the feeders between LP_i and G_j.

A heuristic sequence approach based on the electrical distance is designed and detailed steps are given as follows.

Step 1) Determine the available capacity of G_j during Δt. For μS, G_j is $(1 - \lambda_G \Delta t)G_S$ or $(1 - \lambda_G \Delta t)G_W$, here λ_G is its outage rate; For the transfer point or PCC, G_j is limited by the capacity of feeder.

Step 2) Generate the load recovery sequence for each G_j according to $|Z_{ij}|$. For load points with the same $|Z_{ij}|$, the important one have a higher priority be recovered.

Step 3) If $G_j = 0$, go to step 6; otherwise, go to step 4.

Step 4) If $G_j \geq d_i(1 - x_i\%)$, $G_j = G_j - d_i(1 - x_i\%)$, $x_i\% = 1$ and then go to step 5, here d_i is the load demand of LP_i; otherwise, $x_i\% = x_i\% + G_j/d_i \cdot 100\%$, and go to step 6.

Step 5) $i = i + 1$, or move to the next load point in the sequence of G_j; and then go to step 3.

Step 6) If $j < N_G$ (N_G is the number of alternative power sources), then $j = j + 1$, $i = 1$, and then go to step 3; otherwise, end the process.

C. Short-Term Reliability Indices

Load point requires all components between itself and the power supply point to be operating normally. Consequently, its average short-term outage time ω, average failure rate ξ and outage time r are calculated by (27), (28) and (30) respectively:

$$\begin{bmatrix} \omega_1 \\ \omega_2 \\ \cdots \\ \omega_N \end{bmatrix} = \begin{bmatrix} r_{11} & r_{12} & \cdots & r_{1M} \\ r_{21} & r_{22} & \cdots & r_{2M} \\ \cdots & \cdots & \cdots & \cdots \\ r_{N1} & r_{N2} & \cdots & r_{NM} \end{bmatrix} \cdot \begin{bmatrix} \lambda_1 \\ \lambda_2 \\ \cdots \\ \lambda_M \end{bmatrix} \tag{27}$$

$$\xi_i = \sum_{e=1}^{M} \lambda_e \cdot h(r_{ie}), \quad (i = 1, 2, \ldots, N) \tag{28}$$

$$h(r_{ie}) = \begin{cases} 1, & r_{ie} > 0 \\ 0, & r_{ie} = 0 \end{cases} \tag{29}$$

$$r_i = \frac{\omega_i}{\xi_i}. \tag{30}$$

Short-term reliability indices for microgrid system are defined in line with the ones utilized for distribution system, such as system average interruption frequency index (SAIFI), system average interruption duration index (SAIDI), and energy not supplied index (ENS) [15]. Their corresponding expressions can be described as follows:

$$SAIFI = \sum_{k=1}^{N_\sigma} \left(n(\sigma_k) \cdot \frac{\sum_{i=1}^{N} \xi_i(\sigma_k) \cdot m_i}{\sum_{i=1}^{N} m_i} \right) \tag{31}$$

$$SAIDI = \sum_{k=1}^{N_\sigma} \left(n(\sigma_k) \cdot \frac{\sum_{i=1}^{N} \omega_i(\sigma_k) \cdot m_i}{\sum_{i=1}^{N} m_i} \right) \tag{32}$$

$$ENS = \sum_{k=1}^{N_\sigma} \left(n(\sigma_k) \cdot \frac{\sum_{i=1}^{N} d_i(\sigma_k) \cdot r_i(\sigma_k)}{\sum_{i=1}^{N} m_i} \right) \tag{33}$$

where m_i is the number of customer at LP_i.

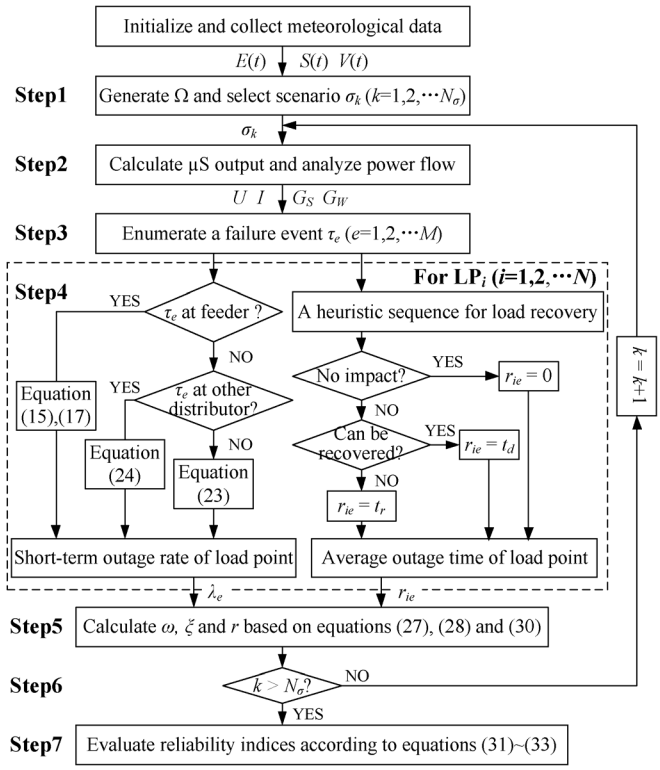

Fig. 7. Flowchart of the evaluation procedure.

D. Solution Process

Enumerative analysis embedded in a heuristic sequence approach is employed to evaluate the operational reliability of the microgrid. The flowchart of the solution process is shown in Fig. 7 and the solution steps are as follows.

Step 1) Generate the scenario set Ω by the grid mesh method in Section II and determine $n(\sigma_k)$ for each scenario.

Step 2) Calculate power outputs of μSs based on meteorological data and analyze power flow.

Step 3) Enumerate M kinds of failure events which contribute to customer failure.

Step 4.1) Calculate the short-term outage rate of feeders and lateral distributors based on the analysis in Section II; then, evaluate their impacts on load points, which is measured by $\lambda_e (e = 1, 2, \ldots M)$.

Step 4.2) Recover from loss of load by using the heuristic sequence approach proposed in Section IV; and then, analyze average outage times of load points according to their classification, as explained in Section IV.

Step 5) Calculate the short-term reliability indices of load points by (27), (28) and (30).

Step 6) Check whether all scenarios have been analyzed.

Step 7) If "No", move to the next scenario; if "Yes", evaluate the short-term reliability indices of microgrid system based on (31)–(33).

V. Case Study

A. Test System

The benchmark system in [16] with some modifications is employed as the test system and detailed distributions will be given in the following sub-sections.

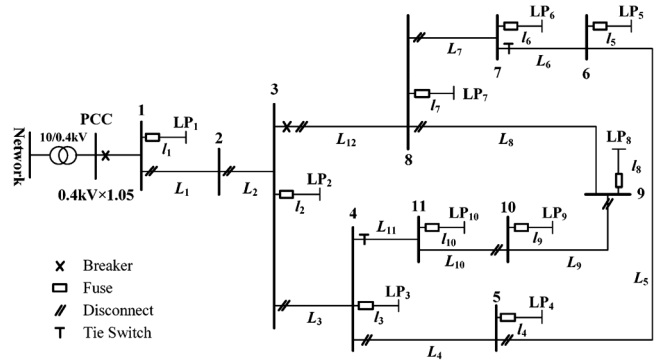

Fig. 8. Benchmark 0.4 kV microgrid network.

TABLE I
Parameters of Main Feeder

No.	R (Ω/km)	X (Ω/km)	C (nF/km)	L (km)	I_N (A)	I_S (A)
L_1	0.579	0.367	9.93	0.282	100	125
L_2	0.164	0.113	413	0.442	100	125
L_3	0.262	0.121	405	0.061	50	63
L_4	0.354	0.129	285	0.056	38	48
L_5	0.336	0.126	343	0.154	38	48
L_6	0.256	0.130	235	0.024	38	48
L_7	0.294	0.123	350	0.167	38	48
L_8	0.339	0.130	273	0.032	50	63
L_9	0.399	0.133	302	0.077	38	48
L_{10}	0.367	0.133	285	0.033	38	48
L_{11}	0.423	0.134	310	0.049	38	48
L_{12}	0.172	0.115	411	0.130	50	63

a) Network: This system comprises 11 nodes, 12 feeders and 10 load points. Fig. 8 shows the one-line diagram of the system, which has two tie lines, L_6 and L_{11}. Feeder parameters are listed in Table I, in which feeder length is reduced to 1/10 of the parameters specified in [16]. For lateral distributors, their lengths are 0.05 km. I_N is set to 30A for l_1 and 25A for others. I_S is set to 60A for l_1 and 50A for others.

Reference voltage is 0.4 kV. ΔU_N and ΔU_S are set to 5% and 10%, respectively.

b) Customer and load data: Table II lists the peak load at each load point. Two typical customer types, namely residential and commercial loads respectively, are simulated and their typical daily load profiles are displayed in Fig. 9.

c) Microsources: Three types of μSs with total capacity of 34 kW are deployed in the system, as described in Table III. Energy storage system does not generate power in grid-connected mode. S_{rate} is 1000 $\mathrm{W/m^2}$. V_{ci}, V_{rate} and V_{co} are set to 2.5 m/s, 10 m/s and 18 m/s, respectively. Annual wind speed and illumination are shown in Fig. 10.

d) Reliability data: Table IV lists the reliability parameters of components. In addition, α is set to 1.6 for ΔU and 1.16 for I, β is 6 and γ is 0.001.

B. System Reliability

In Table V, five cases are designed for comparison: peak load value is used in Case 3 and Case 4; and μS capacity is used

TABLE II
LOAD PARAMETERS

Node No.	Residential		Commercial	
	Load value /kVA	Number of customers	Load value /kVA	Number of customers
1	7.50 +j·1.55	50	2.50+ j·0.50	2
2	—	—	—	—
3	2.76 + j·0.69	50	2.24+ j·1.39	2
4	4.32 + j·1.08	50	—	—
5	7.25 + j·1.82	50	—	—
6	5.50 + j·1.38	50	—	—
7	—	—	0.77+ j·0.48	2
8	5.88 + j·1.47	50	—	—
9	—	—	5.74+ j·3.56	2
10	4.77 + j·1.20	50	0.68+ j·0.42	2
11	3.31 + j·0.83	50	—	—

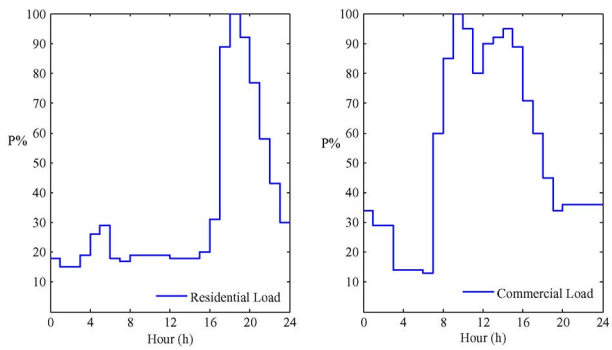

Fig. 9. Typical load profiles: residential load and commercial load.

TABLE III
LOCATIONS AND CAPACITIES OF MICROSOURCES

Node No.	Type of μS	G_{rate} /kW
3	Photovoltaic	4
5	Photovoltaic	5
6	Wind turbine generator	9
8	Energy storage	10
10	Photovoltaic	6

TABLE IV
COMPONENT RELIABILITY DATA

Component (or System)	λ_0	t_r	t_d
Power utility	0.015 /yr	8 h	0.2 h*
Microsources	0.2 /yr	—	0 h
Main feeder	0.1 /yr·km	1 h	0.1 h
Lateral distributor	0.2 /yr·km	1 h	0.01 h**

* is the required time for switching to islanded mode; ** is ΔT_1.

in Case 3. The concept of operating condition here includes two meanings: meteorological condition and load demand with time-varying characteristic.

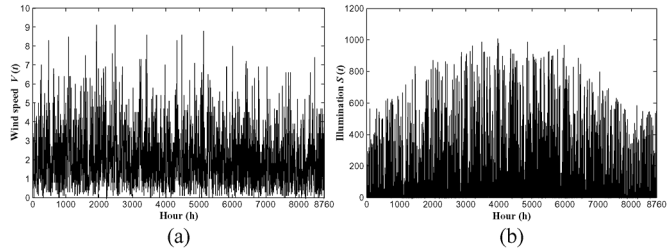

Fig. 10. Annual meteorological data. (a) Wind speed. (b) Illumination.

TABLE V
FIVE CASES UNDER DIFFERENT CONDITIONS

Conditions	Short-term outage model	Operating condition	μSs included
Case 1	Yes	Yes	Yes
Case 2	No	Yes	Yes
Case 3	No	No	Yes
Case 4	No	No	No
Case 5	Yes	Yes	No

TABLE VI
COMPARISON OF SYSTEM RELIABILITY INDICES

Reliability indices	SAIFI (*int/cus-yr*)	SAIDI (*hr/cus-yr*)	ENS (*kWh/yr*)
Case 1	**0.2137**	**0.0963**	**2.2793**
Case 2	0.1684	0.0861	2.1009
Case 3	0.1684	0.0881	4.4586
Case 4	0.1684	0.2070	10.7790
Case 5	0.2426	0.2360	5.1475

The simulation results in Table VI indicate that:

1) SAIFI is determined by component failure rates; therefore, the cases without considering the short-term outage model have the same value for SAIFI, such as Case 2, Case 3 and Case 4. However, SAIFI deteriorates when the protection effect is considered (Case 1 and Case 5). In addition, the interruption frequency in Case 1 is lower than Case 5. This is due to the improvement of power flow distribution caused by adding μSs in Case 1.
2) The μS has a positive effect on the interruption duration and loss of load which can be verified by comparing Case 1 with Case 5, or also the difference between Case 3 and Case 4.
3) Case 3 is related to the conventional approach widely used in microgrid reliability evaluation. Compared with the proposed approach (Case 1), it underestimates the interruption frequency. In addition, it achieves a pessimistic conclusion about ENS owing to the fact that peak values of loads are used.
4) Case 4 corresponds to the distribution network without any μS. More customers inside it are suffering a high risk of outage compared with Case 1. Also, Case 4 underestimates the interruption frequency due to the fact that the effects of protection system are neglected.

TABLE VII
TWO CASES WITH DIFFERENT TYPES OF MICROSOURCES

Conditions	μS type	Meteorological condition	Load
Case 6	PV and WTG	Yes	All commercial
Case 7	All PVs	Yes	All commercial

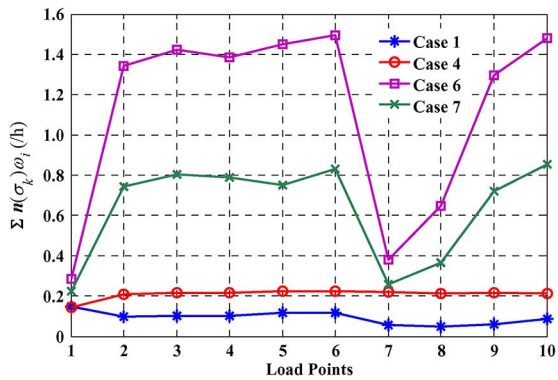

Fig. 11. Average annual outage times of load points in four cases.

C. μS Type

Case 6 and Case 7, as described in Table VII, are designed to investigate the influence of different μS types. The results are compared in Fig. 11.

Some inferences are deduced as follows:

1) Reliability improvement will benefit most of the customers in microgrid according to the comparison between Case 1 and Case 4. However, the development of microgrid has limited effects on load point closed to the main source (i.e., LP_1).
2) Bus No. 8 is selected as the slack bus in the islanded mode. Therefore, customers near this bus can have a relatively high expectation on reliability improvement, such as LP_7 and LP_8 in Case 1, Case 6 and Case 7.
3) Compared with Case 6, Case 7 changes the μS at No. 6 bus from a wind turbine generator to a photovoltaic array. It can be concluded that all customers in Case 7 have better indices. It is because the characteristic of PV output is tightly fitted to the daily load curve of commercial load. In other word, the types of μS should be elaborately designed according to the load profile of each point while planning the microgrid system.

D. Meteorological Condition

The meteorological data given in Fig. 1 and Fig. 10 is collected in H town (Eastern China). If this microgrid is located in G town (Southern China), reliability indices are compared in Fig. 12.

The following conclusions could be easily drawn from this comparative study:

1) Even for microgrids with the identical network, μSs and load demands, we could not expect the same reliability profit. It is because that the operation of microgrid is also related to the meteorological condition at its location.

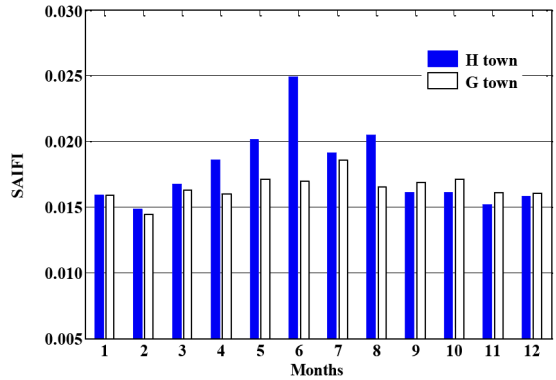

Fig. 12. Monthly indices of SAIFI.

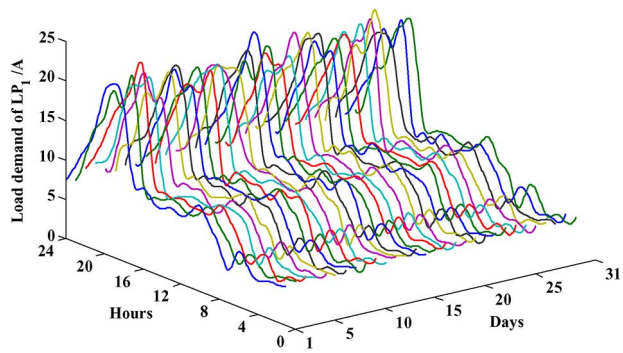

Fig. 13. Monthly load demand of LP_1.

2) The same level of reliability cannot be expected all the year around. As shown in Fig. 12, this microgrid system has the highest reliability in February.

E. Fuse Protection

Fuse may operate when load demand exceeds the capacity of lateral distributor. This subsection will analyze the impacts of load fluctuation on reliability computation. Assuming the load demand is normally distributed as $N(\mu, \varepsilon)$ around the projected demand μ, and the variance ε is set to $\mu/10$, the simulation of LP_1 in one month is given in Fig. 13. In addition, load rate ζ is introduced to reflect the safety margin of lateral distributor

$$\zeta = \frac{\mu}{I_N} \times 100\%. \tag{34}$$

Let λ_1 represent the contribution of fuse action to the average failure rate of LP_1 (ξ_1) and it is calculated by

$$\lambda_1 = \int_{I_N}^{+\infty} \frac{\lambda(I)}{\sqrt{2\pi}\varepsilon} \cdot \exp\left[-\frac{(I-\mu)^2}{2\varepsilon^2}\right] \mathrm{d}I$$
$$\approx \int_{I_N}^{I_S} \frac{I-I_N}{I_S-I_N} \frac{1}{\max\{\Delta T, \Delta t\}} \frac{1}{\sqrt{2\pi}\varepsilon} \exp\left[-\frac{(I-\mu)^2}{2\varepsilon^2}\right] \mathrm{d}I. \tag{35}$$

Subsequently, ξ_1 is evaluated by (28) and its function of ζ and ε is described in Fig. 14. The contours beneath the surface indicate the ranges of ζ and ε to keep ξ_1 in a certain level. For example, If ζ is larger than 0.78 ($\varepsilon = 2.5$ A), the short-term average failure rate of LP_1 reaches 0.0038 /h and then increase significantly. Therefore, a warning that lateral distributor l_1 needs

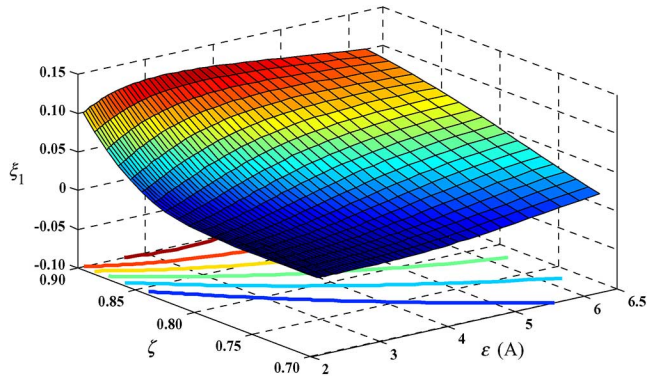

Fig. 14. Average annual outage times of LP_1.

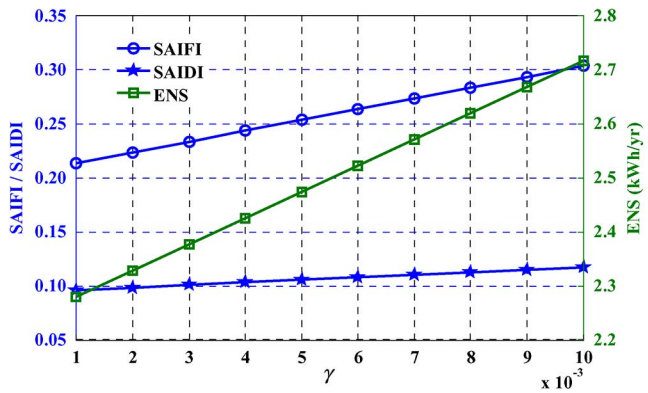

Fig. 15. Relationship between system reliability indices and γ.

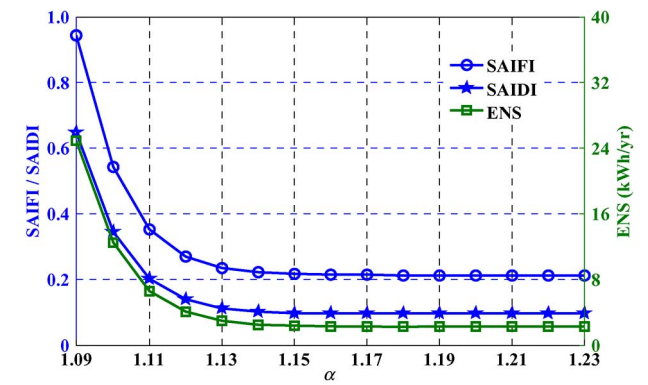

Fig. 16. Relationship between system reliability indices and α.

to be replaced by a line with thicker conductors should be sent to the operator.

F. Protection System

Results in Fig. 15 indicate that system reliability deteriorates along with the increase of reliability factor γ. It is necessary to decrease incorrect probability of protective devices. Otherwise, the benefit of microgrid development on customer reliability will degrade.

To decrease malfunction probability of protection system, x_{set} should have a margin away from x_N, as given in Fig. 16. Furthermore, protection system has no positive effects on reliability improvement on the condition that the repair time is set to the same value for outages caused by various reasons.

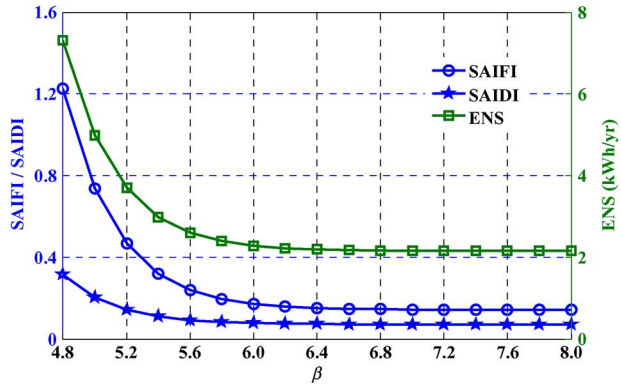

Fig. 17. Relationship between system reliability indices and β.

The results in Fig. 17 imply that system reliability improves as the increase of β. The action zone of the protective device should be limited to a certain range. Otherwise, the outage frequency of customer will increase.

In conclusion, the accuracy, sensitivity and reliability of microgrid protection system need be improved in order to benefit customers inside it.

VI. Conclusion

This paper investigates the reliability evaluation issue in microgrids. The proposed approach is based on a short-term outage model which is specially designed for main feeder and lateral distributor. The evaluation results for the test system demonstrate that both the frequency and the duration of interruptions could be affected by operating conditions. Furthermore, the proposed reliability evaluation strategy provides a feasible solution to quantify the effects of incorrect actions of protection system on the reliability assessment.

However, this paper ignores the diversity of failure effects caused by different factors, such as protection system and random failure. In addition, it was assumed that a component can be repaired in a specified short period without considering whether maintenance work can be carried out or not.

References

[1] P. M. Costa and M. A. Matos, "Assessing the contribution of microgrids to the reliability of distribution networks," *Elect. Power Syst. Res.*, vol. 79, no. 2, pp. 382–389, 2009.

[2] M. E. Khodayar and M. Barati, "Integration of high reliability distribution system in microgrid operation," *IEEE Trans. Smart Grid*, vol. 3, no. 4, pp. 1997–2006, Dec. 2012.

[3] I. S. Bae and J. O. Kim, "Reliability evaluation of distributed generation based on operation mode," *IEEE Trans. Power Syst.*, vol. 22, no. 2, pp. 785–790, May 2007.

[4] I. S. Bae and J. O. Kim, "Reliability evaluation of customers in a microgrid," *IEEE Trans. Power Syst.*, vol. 23, no. 3, pp. 1416–1422, Aug. 2008.

[5] Y. Luo, L. J. Wang, G. Zhu, and G. Wang, "Network analysis and algorithm of microgrid reliability assessment," in *Proc. Power and Energy Engineering Conf. (APPEEC)*, Chengdu, China, Mar. 2010, pp. 1–4.

[6] S. Wang, Z. Li, L. Wu, M. Shahidehpour, and Z. Li, "New metrics for assessing the reliability and economics of microgrids in distribution system," *IEEE Trans. Power Syst.*, to be published.

[7] R. Billinton and G. Bai, "Generating capacity adequacy associated with wind energy," *IEEE Trans. Energy Convers.*, vol. 19, no. 3, pp. 641–646, Sep. 2004.

[8] R. M. Moharil and P. S. Kulkarni, "Reliability analysis of solar photovoltaic system using hourly mean solar radiation data," *Solar Energy*, vol. 84, pp. 691–702, 2010.

[9] J. Mitra and M. R. Vallem, "Determination of storage required to meet reliability guarantees on island-capable microgrids with intermittent sources," *IEEE Trans. Power Syst.*, vol. 27, no. 4, pp. 2360–2367, Nov. 2012.
[10] Z. Bie, P. Zhang, G. Li, B. Hua, M. Meehan, and X. Wang, "Reliability evaluation of active distribution systems including microgrids," *IEEE Trans. Power Syst.*, vol. 27, no. 4, pp. 2342–2350, Nov. 2012.
[11] S. Kennedy, "Reliability evaluation of islanded microgrids with stochastic distributed generation," in *Proc. IEEE Power and Energy Soc. General Meeting*, Calgary, AB, Canada, Jul. 2009, pp. 1–8.
[12] J. He, Y. Z. Sun, P. Wang, and L. Cheng, "A hybrid conditions-dependent outage model of a transformer in reliability evaluation," *IEEE Trans. Power Del.*, vol. 24, no. 4, pp. 2025–2033, Oct. 2009.
[13] E. S. Gavanidou and A. G. Bakirtzis, "Design of a stand alone system with renewable energy sources using trade off methods," *IEEE Trans. Energy Convers.*, vol. 7, no. 1, pp. 42–48, Mar. 1992.
[14] H. Yu, C. Y. Chung, K. P. Wong, and J. H. Zhang, "A chance constrained transmission network expansion planning method with consideration of load and wind farm uncertainties," *IEEE Trans. Power Syst.*, vol. 24, no. 3, pp. 1568–1576, Aug. 2009.
[15] R. Billinton and R. N. Allan, *Reliability Evaluation of Power Systems (Edition 2)*. New York, NY, USA: Plenum, 1996.
[16] K. Rudion, A. Orths, Z. A. Styczynski, and K. Strunz, "Design of benchmark of medium voltage distribution network for investigation of DG integration," in *Proc. Power Engineering Society General Meeting*, Montreal, QC, Canada, Sep. 2006.

Xufeng Xu was born in 1981 in Zhejiang, China. He received the B.E. degree and the Ph.D. degree in electrical engineering from Zhejiang University, Hangzhou, China.

From September 2009 to August 2011, he was a post-doctoral research assistant in the Electrical and Computer Engineering Department at Michigan State University, East Lansing, MI, USA. He is currently working at Tongji University, Shanghai, China. His research interests include power system reliability, power system planning, and microgrid.

Joydeep Mitra (S'94–M'97–SM'02) received the B.Tech. (Hons.) degree in electrical engineering from the Indian Institute of Technology, Kharagpur, India, and the Ph.D. degree in electrical engineering from Texas A&M University, College Station, TX, USA.

He is an Associate Professor of Electrical Engineering at Michigan State University, East Lansing, MI, USA. Prior to this, he was an Associate Professor at New Mexico State University, Las Cruces, NM, USA, Assistant Professor at North Dakota State University, Fargo, ND, USA, and Senior Consulting Engineer at LCG Consulting, Los Altos, CA, USA. His research interests include power system reliability, distributed energy resources, and power system planning.

Tingting Wang (S'11) received the M.E. degree from Zhejiang University, Hangzhou, China. She is currently pursuing the Ph.D. degree in electrical engineering at Clemson University, Clemson, SC, USA.

Her research interest focuses on offshore wind farm switching transient impact on power system.

Longhua Mu received the B.E., M.E., and Ph.D. degrees in electrical engineering from China University of Mining and Technology, Xuzhou, China, in 1986, 1988, and 1998, respectively.

He has been a Full Professor in the Department of Electrical Engineering, Tongji University, Shanghai, China, since 2004. His current research interests include protective relaying of power system, power quality, and microgrid control.